Applied Catalysis B: Environmental 295 (2021) 120319

Contents lists available at ScienceDirect

Applied Catalysis B: Environmental

journal homepage: www.elsevier.com/locate/apcatb

Review

Recent progress in syngas production via catalytic CO_2 hydrogenation reaction

Ali M. Bahmanpour [a], Matteo Signorile [b], Oliver Kröcher [a,c,*]

[a] Institute of Chemical Sciences and Engineering, École Polytechnique Fédérale de Lausanne (EPFL), 1015, Lausanne, Switzerland
[b] Department of Chemistry, NIS Centre and INSTM Reference Center, University of Turin, via P. Giuria 7, 10125, Turin, Italy
[c] Paul Scherrer Institut (PSI), 5232, Villigen, Switzerland

ARTICLE INFO

Keywords:
CO_2 hydrogenation
Reverse water-gas shift reaction
Synthesis gas
Catalyst design

ABSTRACT

Synthesis gas production through the catalytic reverse water-gas shift (RWGS) reaction is an attractive option for the conversion of CO_2 to fuels. Many metal-based catalysts have been introduced for this reaction in order to provide high activity, CO selectivity, and stability. Recently, progress has been made in catalyst design and understanding of the reaction mechanism, which has shed light on the characteristics of the catalysts needed for this reaction. Accordingly, new noble and non-noble metal-based catalysts with remarkable performance have been introduced for this reaction. However, there is still much room for catalyst improvement specifically in regard to catalyst stability at the high temperatures required for this reaction. There are also controversial arguments regarding the active sites of the reaction. This review highlights the recent progress in catalyst design and understanding of the reaction mechanism for the RWGS reaction and derives proposals for further improvements of the process.

1. Introduction

The CO_2 emissions of our modern society into the atmosphere has reached alarming levels, which have led to ocean acidification and climate change [1–3]. These catastrophic consequences have originated the idea to recycle the emitted CO_2 to prevent its accumulation in atmosphere. The recycled CO_2 should be used for the production of value-added bulk chemicals and fuels because the demand for these products is so high that it can use almost all CO_2 emitted from all power plants worldwide and significantly contribute to the solution of the CO_2 problem (Fig. 1a) [4]. However, regarding the established processes in the chemical industry, synthetic fuels and most chemicals are produced from CO and hydrogen (syngas). Processes that use CO_2 directly to form value-added fuels and chemicals as well as their corresponding production plants are missing. Moreover, syngas is currently formed mostly from coal gasification (Fig. 1b). Therefore, production of syngas from recycled CO_2 by means of green hydrogen would be a major step forward to close the carbon loop in the future. In addition to that, synthetic fuels excel by their purity and narrow specifications enabling high engine efficiencies and lower emissions compared to their oil-based counterparts. Some chemicals, such as formic acid, dimethyl ether, methyl formate, and methanol are produced by catalytic CO_2 hydrogenation already today and there have been great improvements in catalyst design for these processes [5–7]. However, CO is still an intermediate in many of these CO_2 hydrogenation processes, such as methanol and DME synthesis [8,9]. The conversion of CO_2 to the intermediate CO needs high temperatures and low pressures unlike the consecutive reaction to methanol and DME. Therefore, formation of CO is not thermodynamically favored at the reaction conditions required for methanol and DME synthesis, which results in low yields of these products in direct CO_2 hydrogenation. A single-step commercial process for the production of methanol/DME from CO_2 has not yet been developed. This behavior reflects the higher reactivity of CO compared to CO_2 and explains the use of CO in the form of syngas for many existing processes in chemical industry such as methanol, higher alcohols or Fischer-Tropsch fuels [10].

The missing link between CO_2 and CO in these processes is known as the reverse water-gas shift (RWGS) reaction (Eq. 1) that allows entering the carbon recycling economy without a fundamental change of the existing infrastructure in chemical industry.

$$CO_2 + H_2 \leftrightarrow CO + H_2O \quad \Delta H = 41.2 \text{kJ.mol}^{-1} \tag{1}$$

Due to the endothermicity of this reaction, CO formation is favorable

* Corresponding author at: Institute of Chemical Sciences and Engineering, École Polytechnique Fédérale de Lausanne (EPFL), 1015, Lausanne, Switzerland.
E-mail address: oliver.kroecher@psi.ch (O. Kröcher).

https://doi.org/10.1016/j.apcatb.2021.120319
Received 17 November 2020; Received in revised form 30 April 2021; Accepted 5 May 2021
Available online 7 May 2021

at high temperatures. This can be also noticed from the changes of the Gibbs free energy with temperature and the increase of the equilibrium constant at higher temperatures [13]. Therefore, relatively high temperatures are required for this reaction, as well as stable catalysts that exhibit high activity and selectivity. However, it is a challenge to design a catalyst, which meets all these criteria, simultaneously. Certain metals supported on metal oxides are known to be highly active and relatively stable in CO_2 hydrogenation reaction producing either CO or CH_4. In particular, Pd, Ru, Rh, Ni and Pt have shown high activity in CO_2 conversion through methanation while others such as Cu, Au, Ag, and Mo are known to selectively produce CO or methanol. Monometallic and bimetallic catalysts seem to perform differently and metal nanoparticle size plays an important role in the CO selectivity. In this review, we will discuss the recent findings on catalyst design and the catalysts performance in the RWGS reaction. We will also review the proposed reaction mechanisms and active sites participating in the RWGS reaction and the controversial findings presented in the literature. By discussing the opportunities and potential improvements, we will conclude this review.

2. Recent advances in catalyst design

High activity and high CO selectivity are among the main criteria for designing a catalyst for the RWGS reaction. Many researchers have recently designed new catalysts with these goals in mind. Table 1 presents some of these recently designed catalysts for the RWGS reaction.

2.1. Selectivity and reactivity of monometallic catalysts

2.1.1. Catalysts with high CO adsorption energy

CO_2 hydrogenation on group 11 transition metals (Cu, Ag, and Au) leads to the formation of CO and/or alcohols and aldehydes through a non-dissociative C—O bond mechanism. This stands in contrast to other studied transition metals, namely Pt, Pd, Ni, Rh, Fe, Co and Ru that tend to form CH_4 due to C—O bond dissociation followed by C—H bond formation [3]. CO is formed on the surface of the catalysts in both cases, which desorbs as final product in case of the RWGS reaction, but is only an intermediate that is further hydrogenated to methane in case of the so-called Sabatier reaction, respectively [3,4]. It is generally accepted that the bond strength of the formed CO on the surface of the metal nanoparticles can determine the product selectivity. Strong interaction of CO with the nanoparticles results in C—O bond dissociation, which helps the formation of CH_4 while weak interaction of CO with the metal nanoparticles results either in desorption of CO as the final product or the formation of alcohols and aldehydes [11,32]. Therefore, we have calculated the adsorption energy of CO on the (1 1 1) surface of various fcc metal nanoparticles, which are investigated in the CO_2 hydrogenation reaction. The (1 1 1) surface is chosen since this is the thermodynamically most stable surface of fcc metals [46]. This is a simplified approach applied in this review only to categorize the monometallic catalysts using a simple but useful descriptor for the observed selectivities. Details of the computational approach can be found in the SI. We have calculated the adsorption energy of CO on Cu, Ag, Au, Pd, Pt, Rh, and Ni. We did not include Ru in our computational set since it is the only non-fcc metal in the series and therefore, its comparison to other metals would be inhomogeneous. However, a strong Ru−CO interaction is already known from other studies [47]. As indicated in Fig. 2, the metal nanoparticles with relatively high CO desorption energy tend to catalyze both the RWGS reaction and the methanation reaction, simultaneously. These metals include Pd, Pt, Ni, and Rh. Ru shows the same behavior when used as monometallic catalyst. CO desorption energy on Ni is relatively lower compared to Rh, Pd, and Pt. However, it is still higher than the group 11 metals (Cu, Au, and Ag) which produce CO selectively. While Ni-based catalysts are well-known for Sabatier reaction, they also form CO as a by-product in most cases [48–52].

Various values for CH_4 and CO selectivity have been reported in the literature using these catalysts [53,54]. However, there are recently studied monometallic catalysts, which can selectively produce CO [32,55]. For example, while Pd is not generally used for the RWGS reaction due to its selectivity towards CH_4, [56,57] monometallic, atomically dispersed Pd/Al_2O_3 was reported to selectively produce CO through CO_2 hydrogenation [8]. It was stated that the difference between atomically dispersed Pd sites supported on Al_2O_3 and Pd clusters can be sought in the active site for CO_2 activation. While CO_2 activation on Al_2O_3 led to the formation of weakly bound CO, which desorbed as the product, activation of CO_2 on Pd clusters formed strongly bound CO, which then was hydrogenated further to form CH_4. Although most supported monometallic Pd clusters have shown to produce CH_4 in a considerable amount, there are catalysts, which have been designed to prove otherwise. SiH supported Pd nanoparticles were shown to selectively produce CO through active participation of SiH in the reaction [55]. Pd catalyzed the dissociative adsorption of H_2 while SiH reacted with CO_2. The reaction mechanism will be presented later in more details. Selective passivation of the CH_4 production sites can also lead to high selectivity towards CO. In a recent study by Du et al., a ZrO_2-Pd-ZrO_2 catalyst was

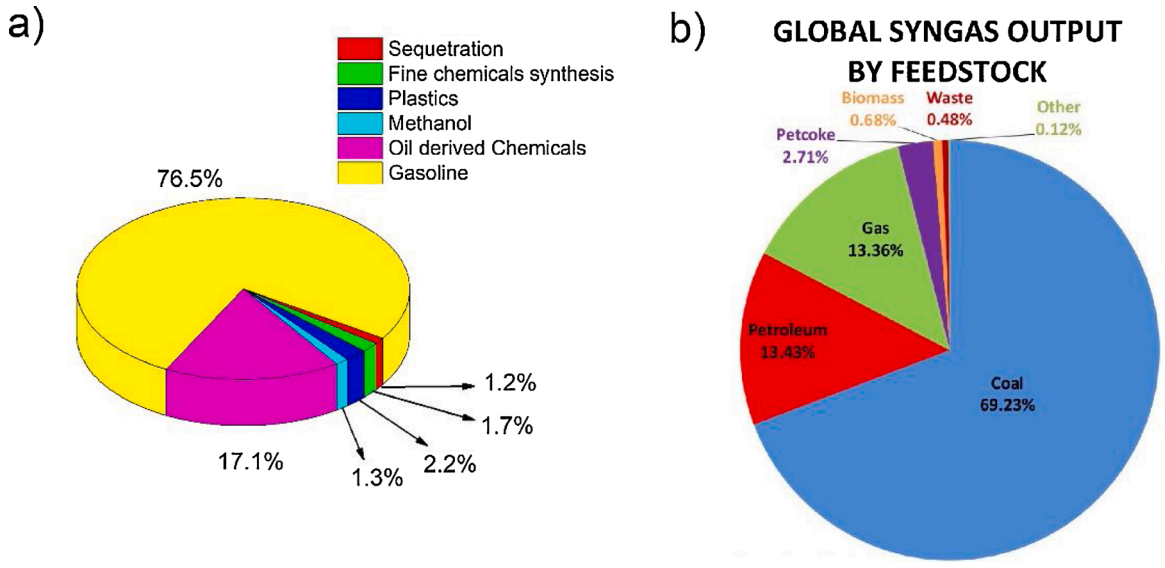

Fig. 1. a) Capacity for CO_2 usage for various industries calculated based on the values given in ref. [11]. b) Sources of syngas production. Figure reproduced form ref [12]. with permission from the Global Syngas Technologies Council. All rights reserved.

Table 1
Summary of reported reaction conditions, CO_2 conversion and CO selectivity for the recent catalysts designed for the RWGS reaction.

Catalyst	H_2:CO_2 molar ratio	Temperature (°C)	Pressure (MPa)	CO_2 Conversion (%)	CO selectivity (%)	WHSV ($L \cdot g_{cat}^{-1} \cdot h^{-1}$)	Ref.
Monometallic catalysts							
Au/Al_2O_3	4:1	400	–	11	100	7.5	[14]
Au/TiO_2	4:1	400	–	35	100	7.5	[14]
Au@UiO-67[a]	3:1	408	2	30	~95	12	[15]
Au/TiO_2	9:1	400	0.1	50	>99	15	[16]
Co/CeO_2	3:1	300	0.1	4	39	36	[17]
Cu/SiO_2	3:1	300	0.1	6	98	1.12*	[18]
Cu/CeO_2	3:1	300	0.1	18	100	1.12*	[18]
Cu/CeO_2-hs	3:1	600	0.1	50	100	300	[19]
CuCe(rod)	4:1	400	0.1	>40	~100	60	[20]
Cu/CeO_2-nanorods	9:1	400	0.1	55	97	30	[21]
Cu/CeO_2-nanocubes	9:1	400	0.1	50	>98	30	[21]
Cs-Cu-CeO_2	9:1	500	0.1	70	>90	30	[22]
Cr_2O_3/Cu	4:1	600	0.1	45	100	150	[23]
8% $Cu/CeO_{2-\delta}$	4:1	400	0.1	2	95	60	[24]
Cu-Mo_2C	4:1	500	–	52	~100	12	[25]
Cs-Mo_2C	4:1	500	–	42	>90	12	[25]
Cu(1)/FAU	1:1	500	0.1	8	98	7.5	[26]
4Cu-Al_2O_3	2:1	600	0.1	47	100	300	[27]
$CuAl_2O_4$	2:1	350	0.1	8	100	15	[28]
Cu/Al_2O_3	3:1	600	0.1	>50	100	–	[29]
1%Cu/ β-Mo_2C	2:1	600	0.1	41	100	300	[30]
5%Ir/CeO_2	4:1	300	1.0	7	> 99	11.4	[31]
20 %Ir/CeO_2	4:1	300	1.0	9	12	11.4	[31]
Pd/SiO_2	1:1	600	0.1	29	82	60	[32]
Pt/CeO_2	1:1	300	0.1	7	–	30	[33]
Pt/SiO_2	2:1	300	0.1	3	100	24.7*	[34]
Pt/TiO_2	2:1	300	0.1	5	99	119.7*	[34]
Pt/mullite	1:1	340	0.1	23	84	27	[35]
Rh@S-1[a]	3:1	500	1.0	52	80	3.6	[36]
Rh@HZSM5[a]	3:1	500	1.0	68	2	3.6	[36]
Rh/S-1	3:1	500	1.0	47	69	3.6	[36]
Bimetallic catalysts							
Au@Pd@UiO-67/Pt@UiO-67[a]	3:1	400	2	36	81	24	[37]
Au@Pd@MOF-74[a]	3:1	400	2	8	~100	24	[38]
Ni_3-Fe_3/ZrO_2	2:1	400	0.1	39	13	9	[39]
Ni_3-Fe_9/ZrO_2	2:1	400	0.1	19	96	9	[39]
Ni-K/Al_2O_3	1:1	700	0.1	~42	<100	15	[40]
Ni-Cu/Saponite	4:1	500	0.1	53	89	15	[41]
NiCo@SiO_2[b]	4:1	850	–	~80	~90	15	[42]
$La_{0.8}K_{0.2}NiO_3$	25:2	300	0.1	~45	<60	48	[43]
Pt-Pd@UiO-67[a]	3:1	400	2	81	18	24	[44]
Pt–Co/TiO_2	2:1	300	–	8	99	36	[45]
Pt–Co/CeO_2	2:1	300	–	9	92	36	[45]
Pt–Co/ZrO_2	2:1	300	–	8	89	36	[45]
K-Pt/mullite	1:1	340	0.1	31	99	27	[35]
Pd-In/SiO_2	1:1	600	0.1	10	100	60	[32]

* Value given in h^{-1}.
[a] Core-shell structure.
[b] Yolk-shell structure.

synthesized using the liquid phase layer deposition technique [58]. Initially, both methanation and the RWGS reaction were observed to take place on the catalyst. However, with time, coke selectively passivated the active sites for CH_4 formation, leading to 100 % selectivity towards CO.

CO_2 hydrogenation on supported Pt has also been reported to produce both CH_4 and CO [59]. As in other studies on previously described noble metals, the catalyst structure plays an important role in determining the product selectivity. While relatively large Pt nanoparticles are known to form CH_4, the active site for CO formation is suggested to be the combination of Pt and the adjacent oxygen vacancy on the support (Pt-O_v) [59,60]. Ni is another metal known to produce methane from CO_2 hydrogenation [61–63]. Ni nanoparticles supported on various metal oxides such as alumina, titania, and ceria-zirconia have been used as the active sites for the methanation reaction [63–66]. However, atomically dispersed Ni sites were found to selectively produce CO as opposed to CH_4 [67]. This remarkable influence of the metal particle size on the selectivity will be discussed below in more detail.

2.1.2. Catalysts with low CO adsorption energy

Unlike metals with strong CO adsorption energy, using monometallic catalysts with weak CO adsorption does not lead to CH_4 formation. For example, Au nanoparticles form methanol [68,69] and CO [70,71] from CO_2, monometallic Au nanoparticles encapsulated in Zr-based MOFs (Au@UiO-67) selectively produce CO, [15] and Au/CeO_2 is an active catalyst for both methanol synthesis and the RWGS reaction [72]. CeO_2 is a well-known reducible catalytic support with the ability to create oxygen vacancies on the surface, [73] but the presence of Au is required for surface reduction [74]. This reduction is easier achieved by using CO as the reducing agent than H_2. It is well known that the presence of oxygen vacancies on the catalyst surface is vital for the catalyst activity in CO_2 hydrogenation reactions [5,75]. Therefore, adding Au to the CeO_2 surface not only increases the ability to form oxygen vacancies by surface reduction, but also creates active sites for H_2 adsorption. Au/CeO_2 is also active for methanol synthesis from CO_2 hydrogenation. In another study, Behm's group demonstrated that while both CO and methanol are initially produced on the Au/CeO_2 surface, inhibition of

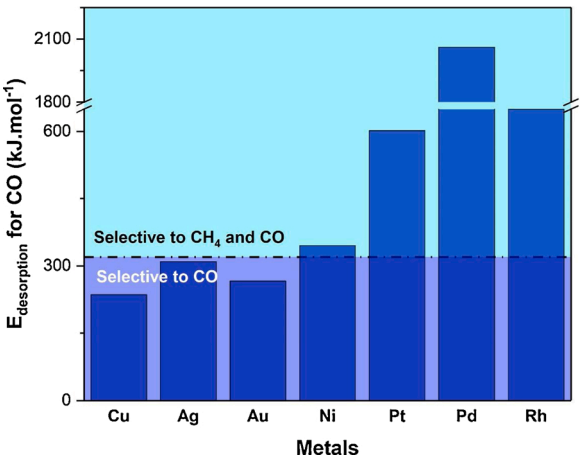

Fig. 2. Calculated CO desorption energies for the (1 1 1) surface of different metals studied for the RWGS and methanation reaction.

the CO formation is faster than methanol, which leads to higher methanol selectivity through the reaction [72]. The catalyst deactivation is proposed to occur through formation of stable carbonate species on the catalyst active sites. The formation of such highly stable carbonates were also observed on other types of catalysts used for the RWGS reaction [28]. Au-based catalysts were are also studied for the RWGS reaction under plasmon-enhanced conditions [70,71]. Huber's group reported more than an order of magnitude improvement in catalyst activity by using localized surface plasmon resonance (LSPR). The decrease in apparent activation energies due to the change in intrinsic reaction kinetics by surface plasmon, as well as the increase in apparent reaction orders due to the decrease in spectator concentration on the catalyst surface, are the main reasons for such improvements in Au-based catalyst activities under plasmon-enhanced conditions.

Copper is another metal with weak CO adsorption energy, which is very well-known for its high selectivity towards CO when used as a catalyst in the CO_2 hydrogenation reaction [76,77]. However, the major drawback of using Cu is its low thermal stability, which leads to fast deactivation of the catalyst particularly at high temperatures. Recently, however, many modifications have been proposed to design highly active and relatively stable copper-based catalysts. Improving the dispersion of copper nanoparticles on β-Mo_2C was shown to have a significant effect on the catalyst stability compared to $Cu/ZnO/Al_2O_3$, a commercial Cu-based catalysts used for WGS reaction [30]. While the initial activity was only slightly improved, the stability was significantly enhanced when compared after 40 h time-on-stream at 600 °C. Cu/β-Mo_2C was found to lose only 15 % of its initial activity while $Cu/ZnO/Al_2O_3$ lost more than 60 %. The same operating conditions were used to test a catalyst with a surface Cu-Al spinel for the RWGS reaction and it was found to be highly stable during the 40 h test with no sign of deactivation [27]. The found formation of Cu-Al spinel oxide on the surface was attributed to the SMSI between isolated Cu^{2+} ions and Al_2O_3. The SMSI between Cu and metal oxides has been linked to the synthesis of other Cu-based catalysts for the RWGS reaction. An inverse nanoporous Cr_2O_3/Cu catalyst was designed by Shen et al., which was found to be active for the RWGS reaction with rates higher than supported noble-metal catalysts [23]. Synthesis of the catalyst was done through de-alloying of CrCuAl alloy forming a Cr_2O_3 layer on nanoporous Cu with high surface area (Fig. 3).

An inverse metal oxide/metal structure has been formed using CeO_2 and copper oxide (forming CeO_2/CuO_x) which has been used for various reactions such as CO oxidation and the WGS reaction [78]. The formation of both Cu^+ and Cu^{2+} in this configuration was reported to be favorable for these reactions [79]. The activity of catalysts for the RWGS reaction is strongly linked to their ability to form oxygen vacancies on their surface. This is demonstrated, for example, by the results of Konsolakis et al. who showed that Cu/CeO_2-nanorods are more active in CO_2 conversion compared with Cu/CeO_2-nanocubes because nanorods have a higher potential in forming oxygen vacancies under reducing conditions [21]. In another example, Chen's group managed to design a highly active Cu/CeO_2 hollow sphere catalyst, which benefits from a high density of oxygen vacancies [19]. This catalyst was tested for the RWGS reaction and proved to be more active than other Cu/CeO_2 catalysts used in the same study with lower oxygen vacancy density. The same conclusions were derived from the work of Zhou et al. [24] They proposed a Cu/CeO_2-δ catalyst, on which Cu° and oxygen vacancies were found to be actively participating in the reaction. The role of oxygen vacancies was proven by comparing Cu-Al and Co-Al spinel oxides as catalysts for the RWGS reaction [28]. The formation of a higher degree of mixed spinel oxides (normal spinel and inverse spinel) in Cu-Al structure forms more oxygen vacancies, which in turn results in higher activity of the Cu-Al spinel oxide compared to the Co-Al one. There are also other spinel-type mixed oxides ($AB_{3-x}O_4$) that are favorable for catalytic reactions due to the formation of defect sites [80]. The role of oxygen vacancies on the spinel oxide surfaces in the RWGS reaction is the adsorption and activation of CO_2 [28,81]. This is supported by CuO/In_2O_3 that was also found to be highly active for the CO_2 reduction due to its ability to form oxygen vacancies, on which CO_2 can be adsorbed and activated [82]. In fact, various factors such as metal particle size, metal-support interaction, metal particle dispersity, and the participation of the support in the reaction can influence the performance of a catalyst. However, the outstanding significance of oxygen vacancies was demonstrated by Jones group, which managed to keep all these variables constant to only monitor the effect of the support on the activity of the supported Cu nanoparticles in the RWGS reaction [18]. They studied Cu/SiO_2 and Cu/CeO_2 with the same above-mentioned characteristics and confirmed, besides the four times higher activity of Cu/CeO_2 than Cu/SiO_2 that the active sites participating in the RWGS reaction on this catalyst are indeed oxygen vacancies and Cu^+.

2.2. Selectivity and reactivity of bimetallic catalysts

As shown above, most monometallic catalysts with high CO adsorption energy favor the formation of CH_4 in CO_2 hydrogenation

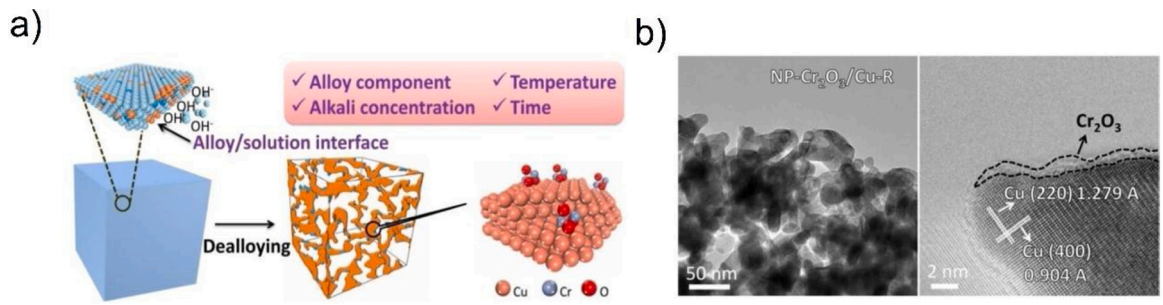

Fig. 3. a) Schematic and b) TEM images of the Cr_2O_3/Cu catalyst reproduced from ref. [21] with permission from Wiley.

reaction while the ones, which weakly adsorb CO, more selectively form CO as the final product. However, using the metals presented in Fig. 2 in bimetallic catalysts can highly affect their activity, stability, and CO selectivity. Recently, it has been shown that Pd-based bimetallic nanoparticles shift the selectivity from the formation of both CH_4 and CO towards higher CO formation. Ye et al. presented a uniformly mixed Pd-In catalyst supported on SiO_2, which can selectively form CO as the CO_2 hydrogenation product [32]. This feature is proposed to be linked to the non-dissociative adsorption of H_2 and weak binding energy of CO while using this bimetallic catalyst. Braga et al. used the same concept of weakening the CO binding energy by synthesizing a bimetallic Ni-Pd catalyst with the direct decomposition method. The catalyst showed much higher selectivity towards CO compared to monometallic Pd, which was synthesized as reference material with the same method [83]. In-situ CO-DRIFTS studies allowed to identify strongly bonded and weakly bonded CO molecules, but only the latter were able to desorb as the final product of the RWGS reaction. Xu's group showed that Au-Pd nanoparticles encapsulated in the structure of the Zn-based and Zr-based MOFs improve the CO selectivity through CO_2 hydrogenation [37,38]. While the reason behind the effect of Au on Pd selectivity towards CO was not discussed, it can be suspected that the higher CO selectivity is caused by the increased electron density of Au in the presence of Pd. The activity of Au nanoparticles for CO_2 adsorption and activation can also be influenced by tuning the Au-metal oxide interface. Yang et al. studied this concept by adding small amounts of CeO_x to Au/TiO_2 [84]. Not only does the addition of CeO_x to Au/TiO_2 help the formation of small Au nanoparticles, which selectively form CO, but it also forms an $Au\text{-}CeO_x\text{-}TiO_2$ interface. While no charge transfer was observed between Au and TiO_2, the addition of CeO_x helped the charge transfer from Au nanoparticles to the support. The electric polarization of the $Au\text{-}CeO_x$ interface helped to form carboxylate species as the intermediate products on the surface of the catalyst, which were then converted to CO and methanol. The main effects of the addition of a second metal or promoter, which have been discussed in the literature, are changes in the electron density or the creation of new active sites. However, other effects such as the change in energy of vacancies formation and the acid/base properties have been also reported as effects caused by the addition of a second metal or promoter [22,85,86]. It should be noted that these effects are related either to the electron density change or the creation of new active sites, i.e. the effects are not completely independent from each other and therefore not further discussed.

The selectivity of bimetallic Ru catalysts can also be shifted towards CO. Le Saché et al. have designed a bimetallic $Ru\text{-}Ni/CeO_2\text{-}ZrO_2$ catalyst, which produces CH_4 or CO depending on the operating temperature [87]. High CH_4 selectivity (93 %) is achieved at low temperatures (350 °C) while at high temperatures (750 °C) the CO selectivity is reported to be 91 %. When Ru is used as promoter, it enhances the activity of already CO-selective catalysts without hampering their selectivity. Simakov group improved the activity of $Cu/ZnO/Al_2O_3$ as a RWGS reaction catalyst by addition of 0.5 % Ru [88]. The catalyst characterization results showed that Ru forms a bond with Cu to convert to a core-shell Ru-Cu nanoparticle. While Ru is usually known as a CH_4-selective catalyst, the increase of the electron density of Ru due to its bond with Cu helps to shift the selectivity from CH_4 to CO.

Pt improves its selectivity to CO in CO_2 hydrogenation by adding a promoter as well. The promoter-Pt interface is regarded as the active site for the RWGS reaction. Huang's group extensively studied the effect of adding K as the promoter to supported Pt-based catalysts [35,89]. They discovered that while Pt catalyzes both the RWGS reaction and the methanation reaction, the addition of K highly increases both the activity and CO selectivity. The K-Pt interface forms active sites for promoting the RWGS reaction, because the strong interaction between Pt nanoparticles and KO_x weakens the adsorption energy of CO on Pt, which inhibits further hydrogenation of CO to form CH_4. Huber's group reported the same effect by adding MoO_x to Pt, [90] which increased the intrinsic activity of a single Pt site at 473 K from 0.4 to 22.7 min^{-1}. Similar to Au, the observed activity increase was explained by a plasmonic effect.

Non-noble metals have been used in bimetallic form to promote the RWGS reaction, too. Chen's group recently discovered that addition of Fe to Ni, which normally promotes the methanation reaction, can form $Ni\text{-}FeO_x$ interfaces, which selectively catalyze CO formation [39]. They discovered that this interface reduces the strength of the M—CO interaction, facilitating the desorption of CO, which in turn increases the CO selectivity. The same effect was found by Varvoutis et al. who reported that while the addition of Cs to Cu/CeO_2 decreased the catalyst activity, it increased the selectivity towards CO [22]. Reina's group reported in another example the positive effect of Cs on the CO selectivity of Fe/Al_2O_3. Besides Cs, they introduced Cu, which enhances the activity and stability of $Fe\text{-}Cu\text{-}Cs/Al_2O_3$ compared to Fe/Al_2O_3, $Fe\text{-}Cu/Al_2O_3$ and $Fe\text{-}Cs/Al_2O_3$ [91]. They reported in their study that while Cs addition enhances the activity and CO selectivity of FeO_x for the RWGS reaction, addition of Cu prevents the FeO_x phase from sintering. The same effect has been reported for Ni promotion by Cu, [41,92] as well as alkali and rare earth metals [40]. Ni promotion by Cu specifically suppresses the methanation reaction to increase CO selectivity [92]. Yolk-shell structures are also commonly used for catalyst stabilization and increased-activity [93,94]. A bimetallic example of such structure used for the RWGS reaction is Ni-promoted Co yolk in an SiO_2 shell. Ni addition promotes the activity of Co as catalyst and helps to form the yolk-shell structure, which is evident from the catalyst characterization results presented by Price et al. [42]

The group 11 transition metals were also used in bimetallic structures for the RWGS reaction. They either have been used as active metals, which become more active by addition of another element, or they act as promoters themselves for shifting the selectivity toward CO. Copper-based catalysts are among the most attractive ones due to the remarkably high CO selectivity of copper. Cu was investigated as a promoter in catalysts with lower initial activity towards CO formation. β-Mo_2C was shown to be able to convert CO_2 to CO through the RWGS reaction. The addition of Cu introduced additional active sites such as Cu° and Cu^{+} on this catalyst, which improved the CO selectivity by about 10 % [25]. Cu was also shown to have an indirect effect on the catalyst activity when used as a promoter. Okemoto et al. found that the addition of Cu to MoO_3/FAU zeolite improved the CO yield. While adding Cu did not seem to increase the number of active sites, the reducibility of MoO_3 to MoO_2 was improved, which resulted in higher CO yield [26]. Therefore, it is generally accepted that not only Cu-based catalysts are active and selective towards CO formation in CO_2 hydrogenation, but also that the addition of Cu as a promoter can increase the CO selectivity of already active catalysts for the CO_2 hydrogenation reaction.

While Cu is preferentially used as the non-noble metal for the RWGS reaction, other non-noble metal-based structures and catalysts have recently attracted the attention of many researchers in this field [95–97]. Carbide structures prepared with metals such as Ti, W and V were found to be active catalysts for the RWGS reaction [98–100]. Rodriguez et al. synthesized M/TiC (M = Au, Cu, Ni) as catalysts for CO_2 hydrogenation. They reported that CO_2 hydrogenation on these catalysts mostly go through HOCO production as an intermediate, which is then hydrogenated to produce CO and only traces of methanol [98]. WC/Al_2O_3 prepared by the evaporation-deposition method was reported by the Willauer group as an active and selective catalyst for the RWGS reaction [99]. They promoted WC/Al_2O_3 with alkali metals such as K and Na. H_2-treated K—WC/Al_2O_3 was found to be more active compared to the one promoted with Na. The catalyst activity, however, was negatively affected by addition of promoters compared to unpromoted WC/Al_2O_3. This effect might be due to the lower BET surface area of the promoted catalyst (87 $m^2\ g^{-1}$ and 95 $m^2 \cdot g^{-1}$ for K promotion and Na promotion, respectively) compared to the unpromoted one (136 $m^2 \cdot g^{-1}$). On the other hand, addition of K and Na boosted the CO

selectivity due to the formation of smaller WC particles. Besides WC/Al_2O_3, the same group also studied 2 % $K\text{-}Mo_2C$ as another carbide-based RWGS catalyst that showed even higher activity [101]. Finally, Pajares et al. proposed VC as active and selective catalyst for the RWGS reaction [100]. Specifically, V_8C_7 was presented in this study and the activity of this catalyst was assigned to the carbon vacancies on the catalyst surface. Similar to oxygen vacancies, the carbon vacancies on V_8C_7 catalyst were used to explain the adsorption and activation of the reactants. The higher density of these vacancies helps to lower the activation energy of CO_2 and H_2 adsorption and the dissociation step.

There are several reasons for the observed shifts in product selectivity and enhancement of the catalyst activity in CO_2 hydrogenation on bimetallic catalysts. In some cases, the structure of the bimetallic catalysts redistributes the local charges and modifies the electron density of the catalyst, which alters the catalyst's performance [102]. In many cases, the charge distribution alters the CO_2 adsorption since the electron-rich site more easily attracts the $C^{\delta+}$ and the electron-deficient site attracts $O^{\delta-}$ as in the case of PtCo bimetallic catalyst [45]. In these cases, the charge transfer is observable from the change of oxidation state of the metals on the catalyst surface. XPS analysis showed that while Ni^{2+} and Co^{3+} are the dominant oxidation states for monometallic Ni and Co catalysts, respectively, the oxidation states of these two ions change to Ni^{3+} and Co^{2+} in a bimetallic NiCo catalyst [103]. Bimetallic catalysts can also enhance the production of the desirable products by addition of an active site. In the case of the K-promoted Pt catalyst, although the presence of KO_x stabilized Pt in its high oxidation state, a new active site, namely $PtKO_x$, was created for decomposition of formate as the intermediate product to form the final products. The same effect was observed by addition of Fe to Ni to form Ni-FeOx as the active sites [39]. This will be discussed in more details in the following section. Hydrogen was found to bind more weakly on the bimetallic transition metal catalysts compared to the corresponding monometallic surfaces [104]. However, the effect of weak hydrogen adsorption on product selectivity has not been fully investigated yet.

2.3. Metal nanoparticle size effect

Like Pd, Ru and Rh strongly adsorb CO as an intermediate in CO_2 hydrogenation. These metals also catalyze CO_2 hydrogenation to form CH_4 [105–111]. However, based on recent studies, new Ru-based catalysts with high selectivity towards CO have been designed. Cargnello's team has discovered that CeO_2 supported Ru catalyst can be tuned to selectively produce either CH_4 or CO [112]. While Ru nanoparticles on CeO_2 selectively produce CH_4 as expected, the nanoparticles decompose into atomically-dispersed Ru on CeO_2 upon reduction, shifting the selectivity completely towards CO. This behavior is reversible, as oxidation leads to the reformation of Ru nanoparticles that produce CH_4 again. The different product selectivity using supported Ru has been tested before through comparison of $5\%Ru/Al_2O_3$ (showing nanoparticles of Ru) and $0.1\ \%Ru/Al_2O_3$ (showing atomic dispersion of Ru) [113]. The former selectively produced CH_4 and the latter produced CO while with time, the atomically-dispersed Ru sintered to form nanoparticles and, accordingly, the selectivity changed to CH_4. It should be noted that the effect of the support on the reaction is more prominent when the metal particle size is small due to the stronger influence of the support in small metal particles. However, with increasing metal particles size the catalyst performance is increasingly dominated by the metal particle characteristics [114].

Matsubu et al. have shown the same effect for Rh/TiO_2 [115]. They have identified Rh nanoparticles and isolated Rh atoms on their catalyst surface. The Rh nanoparticles form CH_4 while isolated atomic Rh sites produce CO. They observed that the nanoparticles disintegrate during reaction into atomically-dispersed isolated Rh sites, which results in a shift of the selectivity towards CO as expected. While many have reported this effect, not many researchers discussed the reason behind such observation. Matsubu et al. explained that the single atom Rh is more likely to form and desorb CO since it is not surrounded with other Rh atoms, which can provide H for further hydrogenation of CO to form CH_4. What we observe is that the active sites for CH_4 formation in these catalysts is a metal-metal entity, whereas the active sites for CO formation are the metal-metal oxide interface. The lower the size of the nanoparticles, the higher the number of metal-metal oxide sites to increase the CO selectivity. It is therefore understandable that atomically dispersed Pd on carbon nanotubes did not produce CO due to the absence of a metal oxide support [8]. Metal-metal oxide sites are also responsible for the increased RWGS activity of K-promoted Pt by forming $Pt\text{-}KO_x$ sites [90]. With this concept, we can also explain the superior activity of materials, such as SiH or $\gamma\text{-}Ga_2O_3$, which adsorb CO_2 and activate hydrogen themselves or are able to diffuse hydrogen from the metal nanoparticle via the interface to far distant CO_2 adsorption sites, where the final product CO is formed. This property differentiates these materials from the above-described metal-metal oxide systems, which require hydrogen activation on the metal sites, from where hydrogen can only spill over to CO_2 adsorption sites in close vicinity to the interface [55,116].

3. Reaction mechanism

3.1. General reaction mechanisms

The RWGS reaction mechanism has been a topic of intensive debate between researchers. Despite the numerous studied catalysts, two reaction mechanisms are most common when searching the literature: First, a redox mechanism, in which H_2 does not participate directly in CO_2 reduction, but reduces the catalyst surface to form H_2O after CO_2 releases one of the oxygen atoms on the catalyst surface (Eq. 2 and 3) [117–119].

$$CO_2 + M - M \rightarrow CO + M - O - M \quad (2)$$

$$H_2 + M - O - M \rightarrow H_2O + M - M \quad (3)$$

The second most common mechanism proposed is the formation of formate as the intermediate product [120–123]. In this mechanism, H_2 directly reacts with CO_2 to form formate on the catalyst surface, followed by further hydrogenation to form CO and H_2O. Here in this section, we will review the recent advances in understanding the RWGS reaction mechanism on various catalysts and the origin of selectivity for this reaction on the catalyst surface.

3.2. Recent advances in understanding the RWGS reaction mechanism

Pd-based catalysts are extensively investigated for this purpose. Pd usually shows both CO and CH_4 formation, which makes it an interesting case for selectivity studies. By investigating two different loadings of Pd on Al_2O_3, the Szanyi group reported that CH_4 and CO are formed on different surface sites [124]. Based on their findings from *in-situ* DRIFTS-MS studies, they noted that Pd/Al_2O_3 works as a bi-functional catalyst. CO_2 is adsorbed on the hydroxyl groups of the Al_2O_3 surface to form formate intermediates while H_2 is dissociatively adsorbed on the Pd nanoparticles. The formed formate species, which are close to the nanoparticles (i.e. at the interface) are further hydrogenated to form CO, which is then transferred to Pd. Two sets of sites for either CO or CH_4 formation are postulated on the Pd surface: Pd sites with weak interaction with CO desorb CO while the ones with strong interaction with CO keep this molecule to hydrogenate it further to produce CH_4 (mechanism is illustrated in Fig. 4). The difference in CO selectivity between catalysts with high and low Pd loading is determined by the concentration of sites, which form strong CO bond.

In a separate study, the Szanyi group reported that the sites with strong CO bond are filled first [125]. Only when these sites are saturated, the sites with weak CO bonds are filled. Therefore, CH_4 formation on Pd/Al_2O_3 is prioritized (Fig. 5). In another study, however, they

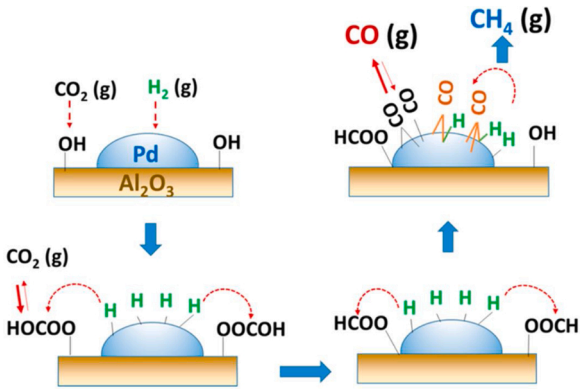

Fig. 4. Illustration of the CO_2 hydrogenation reaction mechanism on Pd/Al_2O_3 reproduced from ref. [124] with permission from the American Chemical Society.

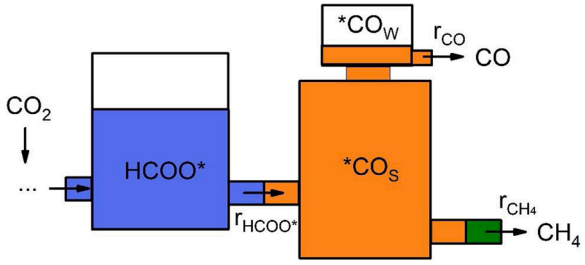

Fig. 5. Illustration of formation of CH_4 and CO from formate. S and W stand for strong and weak adsorption, respectively. Figure is reproduced from ref. [125] with permission from Nature.

claimed that the majority of CO formation on Pd/Al_2O_3 comes from the hydrogenation of carboxyl intermediates, whereas formate molecules only partly participate in this reaction due to their high thermal stability [126]. The formation of formate species is also confirmed on a Pd/Ga_2O_3 catalyst during the RWGS reaction. However, whether formate is formed as a stable species on the catalyst surface or if it reacts as an intermediate product to form CO is difficult to decide with standard spectroscopy techniques. Therefore, Aguirre and Collins used modulation-excitation spectroscopy (MES) combined with phase sensitive detection (PSD) to study the Pd/Ga_2O_3 catalyst surface during H_2 and CO_2 adsorption [116]. Contrary to Al_2O_3, Ga_2O_3 was found to be reduced by H_2 to form Ga-H. The H atoms were transferred from Pd to the Ga_2O_3 support through the spillover effect. Various forms of formate species, namely monodentate, bidentate and bridged formate were formed, out of which, monodentate formate was found to act as the intermediate product that was further hydrogenated to CO.

Unlike Pd/Al_2O_3 and Pd/Ga_2O_3, a redox mechanism is proposed for the RWGS reaction on Pd/SiH by Qian et al [55]. In this study, Si—H bonds were found to be oxidized by CO_2 and form Si—OH and Si—O. CO_2 was therefore reduced to CO. The oxidized surface then accepted H atoms from Pd to desorb water and re-form Si—H bonds.

In general, Pd was found to catalyze CO_2 hydrogenation by dissociative H_2 adsorption upon which either CO or CH_4 are formed and desorbed. Gold nanoparticles in Au/Al_2O_3 were also reported to have a similar role in CO_2 hydrogenation in regard to H_2 dissociation [14]. Surface hydroxyl groups on Al_2O_3 were reported to actively participate in this reaction to form bicarbonate species by their reaction with CO_2. The formed bicarbonate species on the Au-Al_2O_3 interface were claimed to react with atomic H on the Au nanoparticles to form formate. The formates could either decompose to CO and H_2O, or are transferred to other Al_2O_3 surface sites and stay there as spectators. Bobadilla et al. did not consider the presence of oxygen vacancies on Al_2O_3 surface because Al_2O_3 is not a reducible support and therefore, they ruled out the possibility of formation of CO in this way. However, for Pt/Al_2O_3, the prominent role of oxygen vacancies on the Al_2O_3 support in the vicinity of Pt nanoparticles were discussed, where they act as active sites for CO_2 adsorption and activation [60]. On the Au/TiO_2 surface, the situation is more complicated as shown by Bobadilla et al., who reported that Ti^{3+}, oxygen vacancies, as well as hydroxyl groups are active sites for the RWGS reaction, besides the Au nanoparticles. Based on their study, two major mechanisms can be proposed for the RWGS reaction on Au/TiO_2. Either CO_2 can react with the oxygen vacancies to form a carbonate intermediate on the surface, which then reacts with H atoms on the Au nanoparticles as well as the surface hydroxyl groups to form CO and H_2O, or as Rodriguez et al. also proposed for the WGS reaction, [127] CO_2 reacts with adsorbed H atoms on the Au-TiO_2 interface to form a hydroxycarbonyl (OCOH) intermediate, which then decomposes to form CO and a hydroxyl group. The hydroxyl group then reacts with the second H to form and desorb water. These mechanisms are illustrated in Fig. 6.

As mentioned for Au-TiO_2, hydroxycarbonyl or carboxyl species were found to be the intermediate product for CO_2 hydrogenation in various studies [127,128]. Some researchers believe that formate is only formed as a spectator on the catalyst surface while the RWGS reaction in fact takes place through formation of carboxyl groups [129]. Such a carboxyl mechanism, in which CO_2 and H are formed by carboxyl dissociation on the catalyst surface, is discussed for the WGS reaction, making it also a possible pathway for the reverse reaction [130,131]. On Au/CeO_2 however, Behm's group reported the possibility of a redox mechanism for the RWGS reaction [118]. Based on their study, CO_2 has the possibility to release one oxygen atom on the pre-reduced Au/CeO_2 surface, which is the condition for a redox mechanism.

For investigation of the reaction mechanism on Pt, it is important to consider the catalyst morphology as well as the operating conditions. Huang's group reported that while small Pt particles (0–2 nm) favor the formation of CO, CH_4 is formed on the larger nanoparticles (2–5 nm) [59]. Specially with larger nanoparticles, the CO selectivity reduces significantly when operating at higher temperatures compared to lower ones: CO selectivity was > 95 % at 250 °C and ~65 % at 400 °C for the highest loading, which represents the largest Pt nanoparticles. In a separate study, they investigated the role of Pt nanoparticles on CeO_2 for the RWGS reaction [33]. They found that addition of Pt on CeO_2 surface increases the formation of Ce^{3+} sites, which are responsible for CO_2 adsorption. They also discovered that while CO_2 adsorption on Ce^{3+} sites form Ce^{3+}C—O bonds, CO cannot be desorbed without addition of H from an adjacent Pt site. They realized that although the adsorption of CO_2 on the CeO_2 surface resembles a redox mechanism for the RWGS reaction, it actually proceeds via formation of an intermediate formate on the Pt-CeO_2 interface before decomposition to CO and water. Kopač et al. studied the RWGS reaction on the metal surface, interface, and support of a $Cu/SrTiO_3$ catalyst [132]. They reported that formation of CO is favored on the interface of the catalyst and, most importantly, reducing the size of the Cu nanoparticles can boost the activity in the RWGS reaction by increasing the metal-support interface. In agreement with previous studies on the role of Pt, Pd and Au, they concluded that also Cu acts as adsorption sites for H_2 dissociation, providing H atoms for formation of intermediates. However, direct desorption of CO from the catalyst surface without engagement of H_2 was found to be the case for other types of supported copper-based catalysts such as Cu/ β-Mo_2C [30]. Zhang et al. tested their catalyst by exposing it to pulses of CO_2 and monitored the potential CO formation. This is one of the few remarkable examples, which experimentally showed CO formation upon CO_2 dosage without hydrogen. While CO desorption from the catalyst surface was not observed using β-Mo_2C, addition of Cu to the support showed the formation of CO at the moment when CO_2 was introduced to the catalyst in the absence of H_2 at 250 °C (Fig. 7).

While the metal nanoparticles are usually known to act as the hydrogen source for hydrogenation of the adsorbed CO_2 species, Zhang

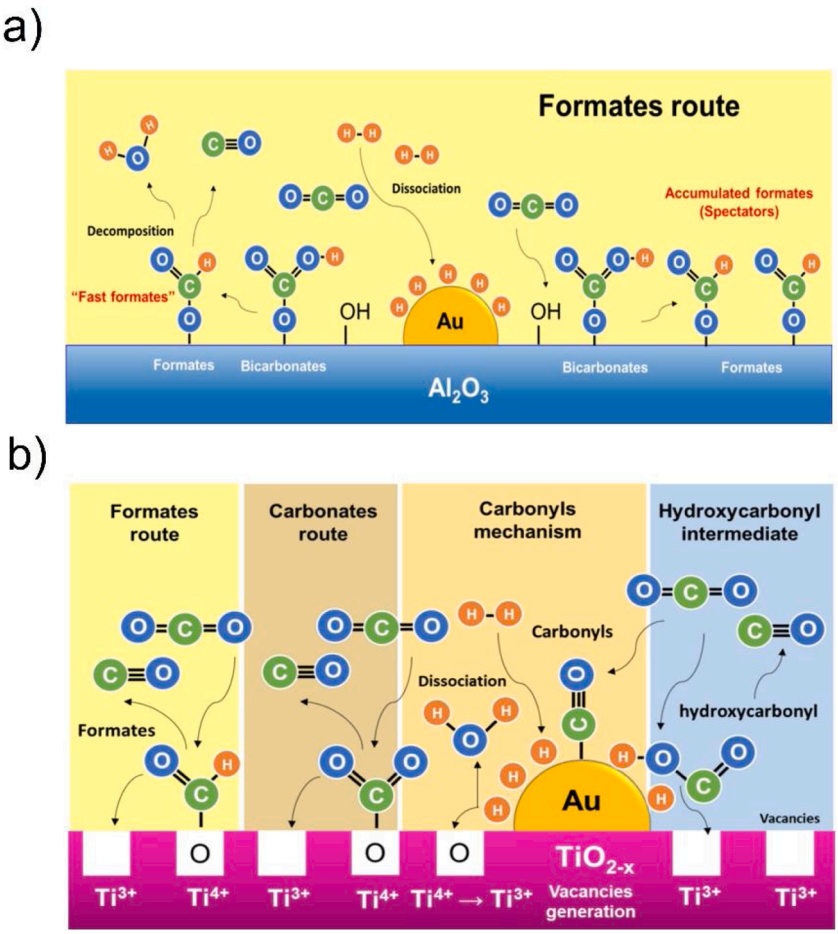

Fig. 6. Proposed reaction mechanism for the RWGS reaction on a) Au/Al_2O_3 and b) Au/TiO_2 reproduced from ref. [14] with permission from the American Chemical Society.

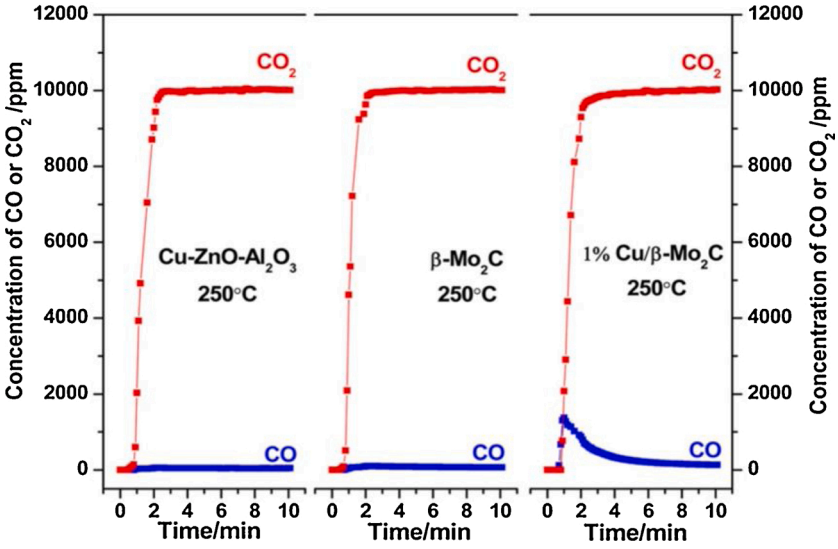

Fig. 7. Dissociation of CO_2 on the catalyst surface without H_2 introduction. Reproduced from ref. [30] with permission from the American Chemical Society.

et al.'s observation and similar studies, which claim a redox mechanism, show that the role of the metal nanoparticles in the RWGS reaction mechanism depends on the structure of the catalyst, the type of support and the presence of hydroxyl groups. The latter will be explained in detail below. Another factor, which has been considered for CO formation is the type of the intermediate, which is formed on the catalyst surface through CO_2 and H_2 adsorption. Schneck et al. showed how the structure of the intermediate could be controlled resulting in a change of catalyst selectivity. Upon normal adsorption of CO_2 on metal hydrides, formates are formed, which are intermediates for forming methanol as

well as formic acid [128]. However, they managed by photochemical manipulation to change the way CO_2 and H_2 were adsorbed, which resulted in the formation of the hydroxycarbonyls as the intermediates for the formation of CO. Other studies also confirmed that the routes for formate formation and CO formation are different. However, unlike Schneck et al., they reported that methanol is formed via the CO formation route [129,133]. Arguments for [14,134] and against [133] the formation of CO from a formate species as an intermediate have been presented in the literature. The main role of the metal nanoparticles as well as the detected potential intermediates on the catalyst surface are therefore yet to be confirmed.

3.3. The effect of hydroxyl groups

As stated above, various reaction mechanisms have been proposed for the formation of CO by CO_2 hydrogenation. However, upon closer inspection, we realized that one of the crucial factors in determining the RWGS reaction mechanism is the presence/absence of the hydroxyl groups on the catalyst surface. This becomes clearer when we investigate the same active metal, Cu for example, in various catalysts structures. When CO_2 adsorption is considered on the Cu (1 0 0), (1 1 0), and (1 1 1) surfaces without support, CO_2 is reduced to CO leaving an oxygen on the Cu surface, [135,136] which is the main step of the redox mechanism. This redox mechanism was proposed by several researchers for unsupported Cu [137] or Cu on metal oxide supports without hydroxyl groups on the suface, such as ZnO or Mo_2C [30,119,138]. However, when Cu is used with supports exposing hydroxyl groups, such as Al_2O_3 or SiO_2, the formation of oxy-hydrogenated intermediate products are reported [120,121]. The same holds for Au as catalyst in the RWGS reaction: on Au/CeO_2 the reaction occurs according to the redox mechanism and on Au/Al_2O_3 the formate mechanism is observed [14, 118]. This has been proven in the theoretical study of Cu/ZnO and Cu/ZnOH for methanol synthesis from CO_2 hydrogenation. Wu et al. discovered that the direct reduction of CO_2 to CO (without hydrogen interaction) is more dominant when Cu/ZnO is used. However, on Cu/ZnOH they discovered that CO_2 hydrogenation to HCOO and CH_3O is promoted showing the effect of the hydroxyl groups on the adsorption of CO_2 [133]. It appears that the surface hydroxyl groups react with the adsorbed CO_2 to form oxygenated species such as formate or bicarbonate, which consequently convert/decompose to CO. Other researchers have confirmed the significant promoting effect of surface hydroxyl groups on CO_2 adsorption and hydrogenation [139,140].

Most studies agree that the metal nanoparticles act as a source of H reservoir for hydrogenation of the intermediate product, which is formed on the metal-support interface. However, some researchers reported that CO can be formed on the catalyst surface through pulsing CO_2 and without direct interference of H_2 [117–119]. Besides the fact, that the mechanism of the RWGS reaction is still controversially discussed, we also have to consider that more than one reaction mechanism might be involved in this reaction and, therefore, a kinetic study can help to identify the prevailing mechanism. For example, parallel cycles for CO_2 adsorption and reaction were detected on the In_2O_3 catalyst surface [141]. Therefore, the mere possibility of CO formation through direct CO_2 reduction on the surface does not necessarily mean that a redox mechanism dominates the reaction. On the other hand, formation of formate and carbonate species have been reported on the catalyst surface. It was found that the majority of the carbonate species formed on the Cu-Al spinel surface upon CO_2 adsorption do not participate in the RWGS reaction [28]. Other researchers reported that formates on the Al_2O_3 surface were found to be adsorbed too strongly to decompose to CO [14]. Therefore, the detection of these compounds cannot be interpreted as proof for their involvement as intermediate products, since they can also be spectators. Specifically, formate, carbonate, and hydrocarboxyl isomers have been proposed as the intermediates in various reports [14,116,128]. However, it is generally accepted that only the intermediates, which form in the vicinity of the H supply, i.e. on the metal-support interface, can contribute to the reaction and the rest of the catalyst surface is not involved in the catalytic cycle. Therefore, increasing the metal-support interface is generally a strategy to increase the activity of a catalyst for the RWGS reaction. Another catalyst feature to consider is its capacity to generate vacancies on the surface. Vacancies have been found to participate in the CO_2 hydrogenation reactions through adsorption of CO_2. Therefore, vacancy creation on the catalyst surface can help the activation of CO_2 molecules if the vacancy is located next to the metal-support interface [60].

4. Conclusions and future opportunities

In this review, we presented the latest findings in the literature on catalyst design and synthesis for the hydrogenation of CO_2 to CO. We also discussed in detail the reaction mechanisms for this reaction. In the following, we summarize the main results of our review:

1- In the search for common properties of catalysts, active for the RWGS reaction, we identified the CO adsorption/desorption energy on the metal surface as useful descriptor to classify their selectivities to CO and CH_4. As an intermediate product before desorption (as CO) or further hydrogenation to CH_4, the strength of the M—CO bond can be used as a criterion for categorizing the metallic nanoparticles that form either CO or CH_4. According to our calculations, metal nanoparticles such as Cu, Au and Ag, which show low tendency to form CH_4 in monometallic catalysts, have a lower CO adsorption energy compared to Pd, Pt, Ni, and Rh.

2- The selectivity of the CO_2 hydrogenation reaction can be strongly influenced by the use of bimetallic catalysts. This implies that the changes in the structure of the active sites, which can affect the strength of the bond between the metal and the intermediate, plays a major role in determining the selectivity in these cases [125,142]. Based on the cases evaluated in the literature, we found that this phenomenon can mainly occur in two ways: One way is the effect of the addition of the second metal on the local charge of the first metal. In this case, the charge transfer may create a scenario for easier adsorption of CO_2 (through creating partial positive and negative charges) or affect the strength of the formed CO on the metal (since metal atoms and ions have different CO adsorption energies). The second way is to create a new active site in the form of metal-metal oxide entities as we have seen in the case of K promoted Pt, were Pt-KO_x was identified as the active site.

3- Significant progress has been achieved recently in understanding the reaction mechanism of the RWGS reaction. In most studies, researchers reported that CO_2 and H_2 form hydrogenated intermediates on the catalyst surface such as formate, carboxylate or bicarbonate. These intermediates then are further hydrogenated/decomposed to form the final products. It is commonly agreed that the intermediate products, which are only formed on the interface of the support and the metal nanoparticles can participate in the reaction, since the adsorbed hydrogen atom on the metal nanoparticle can then react with the intermediate to desorb it as CO and H_2O. Vacancies on the catalyst surface are also generally known to facilitate CO_2 adsorption and activation [28, 100]. Therefore, a catalyst with high concentration of oxygen vacancies as well as weak metal-intermediate bond strength can perform well for the RWGS reaction. Based on the available literature, we propose that the mechanistic differences on the different metal oxide supports can be traced back to the presence or absence of surface hydroxyl groups. Hydroxyl groups adsorb CO_2 to form oxy-hydrogenated intermediate products, whereas in the absence of these hydroxyl groups, CO is formed in a redox mechanism without intermediate formation.

4- Cu-based spinel oxides and spinel-type mixed oxides are particularly promising for CO_2 hydrogenation reactions due to their high activity and stability [81,143]. The observed high activity is caused by a high number of oxygen vacancies and high concentration of Cu^{2+} ions, which can potentially form well-dispersed Cu sites for hydrogen adsorption [27,28,144]. However, the high calcination temperatures that are needed for the formation of this phase leads to the reduction of

the surface area of the active phase, which limits the activity of the catalyst. There are several options to solve this problem. One solution is to stabilize the metals during the calcination process by surface coating, which has been demonstrated very recently [144]. While the surface area can be retained in this method, some deactivation still can be noticed. Another potential solution for hindering the Cu sintering process is to use perovskite structure, which can be reactivated through an oxidation-reduction sequence. These options can be further explored in future studies on catalyst design for the RWGS reaction.

The findings of these studies will be essential for designing potential catalysts, which are not only active, stable, and selective, but also cost effective and suitable for commercialization.

Declaration of Competing Interest

The authors declare that they have no known competing financial interests or personal relationships that could have appeared to influence the work reported in this paper.

Acknowledgment

This research project is part of the Swiss Competence Center for Energy Research SCCER BIOSWEET of the Swiss Innovation Agency Innosuisse. The authors would like to acknowledge the funding provided by EPFL.

Appendix A. Supplementary data

Supplementary material related to this article can be found, in the online version, at doi:https://doi.org/10.1016/j.apcatb.2021.120319.

References

[1] P.M. Cox, R.A. Betts, C.D. Jones, S.A. Spall, I.J. Totterdell, Nature 408 (2000) 184–187.
[2] J.C. Zachos, G.R. Dickens, R.E. Zeebe, Nature 451 (2008) 279–283.
[3] W. Wang, S. Wang, X. Ma, J. Gong, Chem. Soc. Rev. 40 (2011) 3703–3727.
[4] M.D. Porosoff, B. Yan, J.G. Chen, Energy Environ. Sci. 9 (2016) 62–73.
[5] O. Martin, A.J. Martín, C. Mondelli, S. Mitchell, T.F. Segawa, R. Hauert, C. Drouilly, D. Curulla-Ferré, J. Pérez-Ramírez, Angew. Chem. - Int. Ed. 55 (2016) 6261–6265.
[6] F. Studt, I. Sharafutdinov, F. Abild-Pedersen, C.F. Elkjær, J.S. Hummelshøj, S. ø. Dahl, I. Chorkendorff, J.K. Nørskov, Nat. Chem. 6 (2014) 320–324.
[7] A. Álvarez, A. Bansode, A. Urakawa, A.V. Bavykina, T.A. Wezendonk, M. Makkee, J. Gascon, F. Kapteijn, Chem. Rev. 117 (2017) 9804–9838.
[8] J.H. Kwak, L. Kovarik, J. Szanyi, ACS Catal. 3 (2013) 2094–2100.
[9] I.A. Fisher, A.T. Bell, J. Catal. 162 (1996) 54–65.
[10] D.U. Nielsen, X.-M. Hu, K. Daasbjerg, T. Skrydstrup, Nat. Catal. 1 (2018) 244–254.
[11] Y.A. Daza, J.N. Kuhn, RSC Adv. 6 (2016) 49675–49691.
[12] https://www.globalsyngas.org/syngas-production/ Sep. 2020.
[13] C. Callaghan, Kinetics and Catalysis of the Water-Gas-Shift Reaction: A Microkinetic and Graph Theoretic Approach, WORCESTER POLYTECHNIC INSTITUTE, 2006.
[14] L.F. Bobadilla, J.L. Santos, S. Ivanova, J.A. Odriozola, A. Urakawa, ACS Catal. 8 (2018) 7455–7467.
[15] H. Xu, Y. Li, X. Luo, Z. Xu, J. Ge, Chem. Commun. 53 (2017) 7953–7956.
[16] V. Kyriakou, A. Vourros, I. Garagounis, S.A.C. Carabineiro, F.J. Maldonado-Hódar, G.E. Marnellos, M. Konsolakis, Catal. Commun. 98 (2017) 52–56.
[17] M.D. Porosoff, X. Yang, J.A. Boscoboinik, J.G. Chen, Angew. Chem. - Int. Ed. 53 (2014) 6705–6709.
[18] S.-C. Yang, S.H. Pang, T.P. Sulmonetti, W.-N. Su, J.-F. Lee, B.-J. Hwang, C. W. Jones, ACS Catal. 8 (2018) 12056–12066.
[19] Y. Zhang, L. Liang, Z. Chen, J. Wen, W. Zhong, S. Zou, M. Fu, L. Chen, D. Ye, Appl. Surf. Sci. 516 (2020), 146035.
[20] B. Lu, Z. Zhang, X. Li, C. Luo, Y. Xu, L. Zhang, Fuel 276 (2020), 118135.
[21] M. Konsolakis, M. Lykaki, S. Stefa, S.A.C. Carabineiro, G. Varvoutis, E. Papista, G. E. Marnellos, Nanomaterials 9 (2019).
[22] G. Varvoutis, M. Lykaki, E. Papista, S.A.C. Carabineiro, A.C. Psarras, G. E. Marnellos, M. Konsolakis, J. CO2 Util. 44 (2021), 101408.
[23] Y. Shen, Z. Xiao, J. Liu, Z. Wang, ChemCatChem 11 (2019) 5439–5443.
[24] G. Zhou, F. Xie, L. Deng, G. Zhang, H. Xie, Int. J. Hydrog. Energy 45 (2020) 11380–11393.
[25] Q. Zhang, L. Pastor-Pérez, W. Jin, S. Gu, T.R. Reina, Appl. Catal. B Environ. 244 (2019) 889–898.
[26] A. Okemoto, M.R. Harada, T. Ishizaka, N. Hiyoshi, K. Sato, Appl. Catal. Gen. 592 (2020), 117415.
[27] A.M. Bahmanpour, F. Héroguel, M. Kılıç, C.J. Baranowski, L. Artiglia, U. Röthlisberger, J.S. Luterbacher, O. Kröcher, ACS Catal. 9 (2019) 6243–6251.
[28] A.M. Bahmanpour, F. Héroguel, M. Kılıç, C.J. Baranowski, P. Schouwink, U. Röthlisberger, J.S. Luterbacher, O. Kröcher, Appl. Catal. B Environ. 266 (2020), 118669.
[29] S. Choi, B.-I. Sang, J. Hong, K.J. Yoon, J.-W. Son, J.-H. Lee, B.-K. Kim, H. Kim, Sci. Rep. 7 (2017) 41207.
[30] X. Zhang, X. Zhu, L. Lin, S. Yao, M. Zhang, X. Liu, X. Wang, Y.-W. Li, C. Shi, D. Ma, ACS Catal. 7 (2017) 912–918.
[31] S. Li, Y. Xu, Y. Chen, W. Li, L. Lin, M. Li, Y. Deng, X. Wang, B. Ge, C. Yang, S. Yao, J. Xie, Y. Li, X. Liu, D. Ma, Angew. Chem. - Int. Ed. 56 (2017) 10761–10765.
[32] J. Ye, Q. Ge, C.-J. Liu, Chem. Eng. Sci. 135 (2015) 193–201.
[33] X. Chen, X. Su, B. Liang, X. Yang, X. Ren, H. Duan, Y. Huang, T. Zhang, J. Energy Chem. 25 (2016) 1051–1057.
[34] S. Kattel, B. Yan, J.G. Chen, P. Liu, J. Catal. 343 (2016) 115–126.
[35] B. Liang, H. Duan, X. Su, X. Chen, Y. Huang, X. Chen, J.J. Delgado, T. Zhang, Catal. Today 281 (2017) 319–326.
[36] C. Wang, E. Guan, L. Wang, X. Chu, Z. Wu, J. Zhang, Z. Yang, Y. Jiang, L. Zhang, X. Meng, B.C. Gates, F.-S. Xiao, J. Am. Chem. Soc. 141 (2019) 8482–8488.
[37] H. Xu, X. Luo, J. Wang, Y. Su, X. Zhao, Y. Li, ACS Appl. Mater. Interfaces 11 (2019) 20291–20297.
[38] Y. Han, H. Xu, Y. Su, Z.-L. Xu, K. Wang, W. Wang, J. Catal. 370 (2019) 70–78.
[39] B. Yan, B. Zhao, S. Kattel, Q. Wu, S. Yao, D. Su, J.G. Chen, J. Catal. 374 (2019) 60–71.
[40] A. Ranjbar, A. Irankhah, S.F. Aghamiri, Res. Chem. Intermed. 45 (2019) 5125–5141.
[41] N. Nityashree, C.A.H. Price, L. Pastor-Perez, G.V. Manohara, S. Garcia, M. M. Maroto-Valer, T.R. Reina, Appl. Catal. B Environ. 261 (2020), 118241.
[42] C.A.H. Price, L. Pastor-Perez, T.R. Reina, J. Liu, Catal. Today (2020), https://doi.org/10.1016/j.cattod.2020.09.018. In press.
[43] C. Tsounis, Y. Wang, H. Arandiyan, R.J. Wong, C.Y. Toe, R. Amal, J. Scott, Catalysts 10 (2020), 409.
[44] H. Zhang, H. Xu, Y. Li, Y. Su, Appl. Mater. Today 19 (2020), 100609.
[45] S. Kattel, W. Yu, X. Yang, B. Yan, Y. Huang, W. Wan, P. Liu, J.G. Chen, Angew. Chem. - Int. Ed. 55 (2016) 7968–7973.
[46] A. Patra, S. Jana, L.A. Constantin, L. Chiodo, P. Samal, J. Chem. Phys. 152 (2020), 151101.
[47] I.M. Ciobica, A.W. Kleyn, R.A. Van Santen, J. Phys. Chem. B 107 (2003) 164–172.
[48] G. Garbarino, P. Riani, L. Magistri, G. Busca, Int. J. Hydrog. Energy 39 (2014) 11557–11565.
[49] R. Mutschler, E. Moioli, W. Luo, N. Gallandat, A. Züttel, J. Catal. 366 (2018) 139–149.
[50] H.-C. Wu, T.-C. Chen, J.-H. Wu, C.-W. Pao, C.-S. Chen, J. Colloid Interface Sci. 586 (2021) 514–527.
[51] A.R. Richard, M. Fan, ACS Catal. 7 (2017) 5679–5692.
[52] H.C. Wu, Y.C. Chang, J.H. Wu, J.H. Lin, I.K. Lin, C.S. Chen, Catal. Sci. Technol. 5 (2015) 4154–4163.
[53] M. Younas, L. Loong Kong, M.J.K. Bashir, H. Nadeem, A. Shehzad, S. Sethupathi, Energy Fuels 30 (2016) 8815–8831.
[54] S. Rönsch, J. Schneider, S. Matthischke, M. Schlüter, M. Götz, J. Lefebvre, P. Prabhakaran, S. Bajohr, Fuel 166 (2016) 276–296.
[55] C. Qian, W. Sun, D.L.H. Hung, C. Qiu, M. Makaremi, S.G. Hari Kumar, L. Wan, M. Ghoussoub, T.E. Wood, M. Xia, A.A. Tountas, Y.F. Li, L. Wang, Y. Dong, I. Gourevich, C.V. Singh, G.A. Ozin, Nat. Catal. 2 (2019) 46–54.
[56] A. Erdöhelyi, M. Pásztor, F. Solymosi, J. Catal. 98 (1986) 166–177.
[57] A. Karelovic, P. Ruiz, ACS Catal. 3 (2013) 2799–2812.
[58] Y.-P. Du, A.M. Bahmanpour, L. Milosevic, F. Héroguel, M. Mensi, O. Kröcher, J. S. Luterbacher, ACS Catal. (2020) 12058–12070.
[59] X. Chen, X. Su, H. Duan, B. Liang, Y. Huang, T. Zhang, Catal. Today 281 (2017) 312–318.
[60] D. Ferri, T. Bürgi, A. Baiker, Phys. Chem. Chem. Phys. 4 (2002) 2667–2672.
[61] J. Gödde, M. Merko, W. Xia, M. Muhler, J. Energy Chem. 54 (2021) 323–331.
[62] X. Xu, Y. Tong, J. Huang, J. Zhu, X. Fang, J. Xu, X. Wang, Fuel 283 (2021), 118867.
[63] P. Unwiset, K.C. Chanapattharapol, P. Kidkhunthod, Y. Poo-arporn, B. Ohtani, Chem. Eng. Sci. 228 (2020), 115955.
[64] L. Xu, X. Wen, M. Chen, C. Lv, Y. Cui, X. Wu, C.-E. Wu, B. Yang, Z. Miao, X. Hu, Fuel 282 (2020), 118813.
[65] L. Proaño, M.A. Arellano-Treviño, R.J. Farrauto, M. Figueredo, C. Jeong-Potter, M. Cobo, Appl. Surf. Sci. 533 (2020), 147469.
[66] G. Varvoutis, M. Lykaki, S. Stefa, E. Papista, S.A.C. Carabineiro, G.E. Marnellos, M. Konsolakis, Catal. Commun. 142 (2020), 106036.
[67] Y. Hou, Y.-L. Liang, P.-C. Shi, Y.-B. Huang, R. Cao, Appl. Catal. B Environ. 271 (2020), 118929.
[68] H. Sakurai, M. Haruta, Catal. Today 29 (1996) 361–365.
[69] J.A. Rodriguez, P. Liu, D.J. Stacchiola, S.D. Senanayake, M.G. White, J.G. Chen, ACS Catal. 5 (2015) 6696–6706.
[70] I. Ro, R. Carrasquillo-Flores, J.A. Dumesic, G.W. Huber, Appl. Catal. Gen. 521 (2016) 182–189.
[71] A.A. Upadhye, I. Ro, X. Zeng, H.J. Kim, I. Tejedor, M.A. Anderson, J.A. Dumesic, G.W. Huber, Catal. Sci. Technol. 5 (2015) 2590–2601.
[72] A. Rezvani, A.M. Abdel-Mageed, T. Ishida, T. Murayama, M. Parlinska-Wojtan, R. J. Behm, ACS Catal. 10 (2020) 3580–3594.

[73] A.R. Puigdollers, P. Schlexer, S. Tosoni, G. Pacchioni, ACS Catal. 7 (2017) 6493–6513.
[74] L.C. Wang, D. Widmann, R.J. Behm, Catal. Sci. Technol. 5 (2015) 925–941.
[75] J. Ye, C. Liu, D. Mei, Q. Ge, ACS Catal. 3 (2013) 1296–1306.
[76] S. Saeidi, S. Najari, F. Fazlollahi, M.K. Nikoo, F. Sefidkon, J.J. Klemeš, L.L. Baxter, Renew. Sustain. Energy Rev. 80 (2017) 1292–1311.
[77] M. Konsolakis, Appl. Catal. B Environ. 198 (2016) 49–66.
[78] M. Konsolakis, M. Lykaki, Catalysts 10 (2020).
[79] Y. Xie, Y. Yin, S. Zeng, M. Gao, H. Su, Catal. Commun. 99 (2017) 110–114.
[80] C. Yuan, H.B. Wu, Y. Xie, X.W. Lou, Angew. Chem. - Int. Ed. 53 (2014) 1488–1504.
[81] X. Liu, M. Wang, C. Zhou, W. Zhou, K. Cheng, J. Kang, Q. Zhang, W. Deng, Y. Wang, Chem. Commun. 54 (2017) 140–143.
[82] P. Devi, K. Malik, E. Arora, S. Bhattacharya, V. Kalendra, K.V. Lakshmi, A. Verma, J.P. Singh, Catal. Sci. Technol. 9 (2019) 5339–5349.
[83] A.H. Braga, N.J.S. Costa, K. Philippot, R.V. Gonçalves, J. Szanyi, L.M. Rossi, ChemCatChem (2020) 2967–2976.
[84] X. Yang, S. Kattel, S.D. Senanayake, J.A. Boscoboinik, X. Nie, J. Graciani, J. A. Rodriguez, P. Liu, D.J. Stacchiola, J.G. Chen, J. Am. Chem. Soc. 137 (2015) 10104–10107.
[85] Q. Tan, Z. Shi, D. Wu, Ind. Eng. Chem. Res. 57 (2018) 10148–10158.
[86] L. Guo, Y. Cui, H. Li, Y. Fang, R. Prasert, J. Wu, G. Yang, Y. Yoneyama, N. Tsubaki, Catal. Commun. 130 (2019), 105759.
[87] E. Le Saché, L. Pastor-Pérez, B.J. Haycock, J.J. Villora-Picó, A. Sepúlveda-Escribano, T.R. Reina, ACS Sustain. Chem. Eng. 8 (2020) 4614–4622.
[88] Y. Zhuang, R. Currie, K.B. McAuley, D.S.A. Simakov, Appl. Catal. Gen. 575 (2019) 74–86.
[89] X. Yang, X. Su, X. Chen, H. Duan, B. Liang, Q. Liu, X. Liu, Y. Ren, Y. Huang, T. Zhang, Appl. Catal. B Environ. 216 (2017) 95–105.
[90] I. Ro, C. Sener, T.M. Stadelman, M.R. Ball, J.M. Venegas, S.P. Burt, I. Hermans, J. A. Dumesic, G.W. Huber, J. Catal. 344 (2016) 784–794.
[91] L. Pastor-Pérez, F. Baibars, E. Le Sache, H. Arellano-García, S. Gu, T.R. Reina, J. CO2 Util. 21 (2017) 423–428.
[92] O. Arbeláez, T.R. Reina, S. Ivanova, F. Bustamante, A.L. Villa, M.A. Centeno, J. A. Odriozola, Appl. Catal. Gen. 497 (2015) 1–9.
[93] C.A.H. Price, T.R. Reina, J. Liu, J. Energy Chem. 57 (2021) 304–324.
[94] R.-P. Ye, X. Wang, C.-A.H. Price, X. Liu, Q. Yang, M. Jaroniec, J. Liu, Small 17 (2021), 1906250.
[95] L. Pastor-Pérez, M. Shah, E. Le Saché, T.R. Reina, Catalysts 8 (2018), 608.
[96] D.H. Kim, S.W. Han, H.S. Yoon, Y.D. Kim, J. Ind. Eng. Chem. 23 (2015) 67–71.
[97] S. Sengupta, A. Jha, P. Shende, R. Maskara, A.K. Das, J. Environ. Chem. Eng. 7 (2019), 102911.
[98] J.A. Rodriguez, J. Evans, L. Feria, A.B. Vidal, P. Liu, K. Nakamura, F. Illas, J. Catal. 307 (2013) 162–169.
[99] J.R. Morse, M. Juneau, J.W. Baldwin, M.D. Porosoff, H.D. Willauer, J. CO2 Util. 35 (2020) 38–46.
[100] A. Pajares, H. Prats, A. Romero, F. Viñes, P.R. de la Piscina, R. Sayós, N. Homs, F. Illas, Appl. Catal. B Environ. 267 (2020), 118719.
[101] M.D. Porosoff, J.W. Baldwin, X. Peng, G. Mpourmpakis, H.D. Willauer, ChemSusChem 10 (2017) 2408–2415.
[102] C. Xu, A. Vasileff, B. Jin, D. Wang, H. Xu, Y. Zheng, S.-Z. Qiao, Chem. Commun. 56 (2020) 11275–11278.
[103] M. Koehle, A. Mhadeshwar, in: S.L. Suib (Ed.), New Future Dev. Catal., Elsevier, Amsterdam, 2013, pp. 63–93.
[104] A.M. Goda, M.A. Barteau, J.G. Chen, J. Phys. Chem. B 110 (2006) 11823–11831.
[105] M. Fan, J.D. Jimenez, S.N. Shirodkar, J. Wu, S. Chen, L. Song, M.M. Royko, J. Zhang, H. Guo, J. Cui, K. Zuo, W. Wang, C. Zhang, F. Yuan, R. Vajtai, J. Qian, J. Yang, B.I. Yakobson, J.M. Tour, J. Lauterbach, D. Sun, P.M. Ajayan, ACS Catal. 9 (2019) 10077–10086.
[106] A. Porta, L. Falbo, C.G. Visconti, L. Lietti, C. Bassano, P. Deiana, Catal. Today 343 (2020) 38–47.
[107] H. Wu, M. Yuan, J. Huang, X. Li, Y. Wang, J. Li, Z. You, Appl. Catal. Gen. 595 (2020), 117474.
[108] F. Wang, S. He, H. Chen, B. Wang, L. Zheng, M. Wei, D.G. Evans, X. Duan, J. Am. Chem. Soc. 138 (2016) 6298–6305.
[109] T. Abe, M. Tanizawa, K. Watanabe, A. Taguchi, Energy Environ. Sci. 2 (2009) 315–321.
[110] S. Sharma, Z. Hu, P. Zhang, E.W. McFarland, H. Metiu, J. Catal. 278 (2011) 297–309.
[111] A.M. Abdel-Mageed, K. Wiese, M. Parlinska-Wojtan, J. Rabeah, A. Brückner, R. J. Behm, Appl. Catal. B Environ. 270 (2020), 118846.
[112] A. Aitbekova, L. Wu, C.J. Wrasman, A. Boubnov, A.S. Hoffman, E.D. Goodman, S. R. Bare, M. Cargnello, J. Am. Chem. Soc. 140 (2018) 13736–13745.
[113] J.H. Kwak, L. Kovarik, J. Szanyi, ACS Catal. 3 (2013) 2449–2455.
[114] G. Pacchioni, Phys. Chem. Chem. Phys. 15 (2013) 1737–1757.
[115] J.C. Matsubu, V.N. Yang, P. Christopher, J. Am. Chem. Soc. 137 (2015) 3076–3084.
[116] A. Aguirre, S.E. Collins, Catal. Today 205 (2013) 34–40.
[117] M.J.L. Ginés, A.J. Marchi, C.R. Apesteguía, Appl. Catal. Gen. 154 (1997) 155–171.
[118] L.C. Wang, M. Tahvildar Khazaneh, D. Widmann, R.J. Behm, J. Catal. 302 (2013) 20–30.
[119] S.-I. Fujita, M. Usui, N. Takezawa, J. Catal. 134 (1992) 220–225.
[120] C.-S. Chen, W.-H. Cheng, S.-S. Lin, Catal. Lett. 68 (2000) 45–48.
[121] C.-S. Chen, W.-H. Cheng, Catal. Lett. 83 (2002) 121–126.
[122] C.S. Chen, J.H. Wu, T.W. Lai, J. Phys. Chem. C 114 (2010) 15021–15028.
[123] N. Ishito, K. Hara, K. Nakajima, A. Fukuoka, J. Energy Chem. 25 (2016) 306–310.
[124] X. Wang, H. Shi, J.H. Kwak, J. Szanyi, ACS Catal. 5 (2015) 6337–6349.
[125] X. Wang, H. Shi, J. Szanyi, Nat. Commun. 8 (2017) 513.
[126] N.C. Nelson, M.-T. Nguyen, V.-A. Glezakou, R. Rousseau, J. Szanyi, Nat. Catal. 2 (2019) 916–924.
[127] J.A. Rodríguez, J. Evans, J. Graciani, J.-B. Park, P. Liu, J. Hrbek, J.Fdez. Sanz, J. Phys. Chem. C 113 (2009) 7364–7370.
[128] F. Schneck, J. Ahrens, M. Finger, A.C. Stückl, C. Würtele, D. Schwarzer, S. Schneider, Nat. Commun. 9 (2018), 1161.
[129] S. Kattel, B. Yan, Y. Yang, J.G. Chen, P. Liu, J. Am. Chem. Soc. 138 (2016) 12440–12450.
[130] E. Baraj, K. Ciahotný, T. Hlinčík, Fuel 288 (2021), 119817.
[131] J.L.C. Fajín, M.N.D.S. Cordeiro, Appl. Surf. Sci. 542 (2021), 148589.
[132] D. Kopač, B. Likozar, M. Huš, ACS Catal. 10 (2020) 4092–4102.
[133] X.-K. Wu, G.-J. Xia, Z. Huang, D.K. Rai, H. Zhao, J. Zhang, J. Yun, Y.-G. Wang, Appl. Surf. Sci. 525 (2020), 146481.
[134] T.-Y. Chen, C. Cao, T.-B. Chen, X. Ding, H. Huang, L. Shen, X. Cao, M. Zhu, J. Xu, J. Gao, Y.-F. Han, ACS Catal. 9 (2019) 8785–8797.
[135] B. Eren, R.S. Weatherup, N. Liakakos, G.A. Somorjai, M. Salmeron, J. Am. Chem. Soc. 138 (2016) 8207–8211.
[136] G.-C. Wang, J. Nakamura, J. Phys. Chem. Lett. 1 (2010) 3053–3057.
[137] R.A. Hadden, H.D. Vandervell, K.C. Waugh, G. Webb, Catal. Lett. 1 (1988) 27–33.
[138] Y. Cui, G. Wang, Y. Sun, B. Zhong, J. Fuel Chem. Technol. 25 (1997) 388.
[139] P. Hongmanorom, J. Ashok, G. Zhang, Z. Bian, M.H. Wai, Y. Zeng, S. Xi, A. Borgna, S. Kawi, Appl. Catal. B Environ. 282 (2021).
[140] H. Kusama, K.K. Bando, K. Okabe, H. Arakawa, Appl. Catal. Gen. 205 (2001) 285–294.
[141] J. Wang, C.-Y. Liu, T.P. Senftle, J. Zhu, G. Zhang, X. Guo, C. Song, ACS Catal. 10 (2020) 3264–3273.
[142] S. Kattel, P. Liu, J.G. Chen, J. Am. Chem. Soc. 139 (2017) 9739–9754.
[143] O.-S. Joo, K.-D. Jung, Bull. Korean Chem. Soc. 24 (2003) 86–90.
[144] A.M. Bahmanpour, B.P. Le Monnier, Y.-P. Du, F. Héroguel, J.S. Luterbacher, O. Kröcher, Chem. Commun. 57 (2021) 1153–1156.